JHEP

Published for SISSA by Springer

Received: March 9, 2020
Revised: April 3, 2020
Accepted: April 16, 2020
Published: May 4, 2020

QCD θ-vacuum energy and axion properties

Zhen-Yan Lu,[a,b] **Meng-Lin Du,**[c] **Feng-Kun Guo,**[b,d] **Ulf-G. Meißner**[c,e,f] **and Thomas Vonk**[c]

[a] *School of Physics and Electronic Science, Hunan University of Science and Technology, Xiangtan 411201, China*

[b] *CAS Key Laboratory of Theoretical Physics, Institute of Theoretical Physics, Chinese Academy of Sciences, Beijing 100190, China*

[c] *Helmholtz-Institut für Strahlen- und Kernphysik and Bethe Center for Theoretical Physics, Universität Bonn, D-53115 Bonn, Germany*

[d] *School of Physical Sciences, University of Chinese Academy of Sciences, Beijing 100049, China*

[e] *Institute for Advanced Simulation, Institut für Kernphysik and Jülich Center for Hadron Physics, Forschungszentrum Jülich, D-52425 Jülich, Germany*

[f] *Tbilisi State University, 0186 Tbilisi, Georgia*

E-mail: luzhenyan@hnust.edu.cn, du@hiskp.uni-bonn.de, fkguo@itp.ac.cn, meissner@hiskp.uni-bonn.de, vonk@hiskp.uni-bonn.de

Abstract: At low energies, the strong interaction is governed by the Goldstone bosons associated with the spontaneous chiral symmetry breaking, which can be systematically described by chiral perturbation theory. In this paper, we apply this theory to study the θ-vacuum energy density and hence the QCD axion potential up to next-to-leading order with N non-degenerate quark masses. By setting $N = 3$, we then derive the axion mass, self-coupling, topological susceptibility and the normalized fourth cumulant both analytically and numerically, taking the strong isospin breaking effects into account. In addition, the model-independent part of the axion-photon coupling, which is important for axion search experiments, is also extracted from the chiral Lagrangian supplemented with the anomalous terms up to $\mathcal{O}(p^6)$.

Keywords: Beyond Standard Model, Chiral Lagrangians, Effective Field Theories

ArXiv ePrint: 2003.01625

https://doi.org/10.1007/JHEP05(2020)001

JHEP05(2020)001

Contents

JHEP05(2020)001

1 Introduction

A CP-violating topological term, i.e., the θ-term, is allowed in the Quantum Chromodynamics (QCD) Lagrangian. It can be written as

$$\mathcal{L}_\theta = \theta_0 \frac{\alpha_s}{8\pi} G^{\mu\nu,c} \tilde{G}^c_{\mu\nu}, \tag{1.1}$$

where α_s is the QCD coupling constant, $G^{\mu\nu,c}$ is the gluon field strength tensor, with c a color index, and $\tilde{G}^c_{\mu\nu} = \varepsilon_{\mu\nu\rho\sigma} G^{\rho\sigma,c}/2$ its dual. Because none of the quarks is massless, physical observables only depend on a combination of the θ_0 parameter and the phases present in the quark mass matrix $\mathcal{M}_q$, i.e., $\theta = \theta_0 + \arg\det\mathcal{M}_q$. Being a dimensionless parameter, the natural value of θ is expected to be $\mathcal{O}(1)$, which would significantly affect physical systems such as atomic nuclei, and lead to measurable effects, as nucleons, for instance, would possess a nonvanishing electric dipole moment [1]. However, the so-far negative results of experimental searches for the nucleon electric dipole moment lead to a tiny upper limit: $|\theta| \lesssim 10^{-10}$ [2–7]. To understand why the value of θ is so small is the so-called *strong CP problem*. One elegant possible solution of this problem is the Peccei-Quinn (PQ) mechanism [8, 9], which introduces a global U(1) symmetry, called PQ symmetry. This symmetry is spontaneously broken at energies much higher than the typical QCD scale of order $\mathcal{O}(1\,\mathrm{GeV})$ and is also broken by an anomalous coupling to gluon fields. The axion appears as the corresponding Goldstone boson [10, 11] which has an anomalous coupling to $G\tilde{G}$. The parameter θ is then dynamically driven to zero at the minimum of the axion potential, giving rise to a possible solution to the strong CP problem.

In the past few decades, there have been tremendous efforts searching for the axion, denoted by a, as well as constraining to its mass m_a and decay constant f_a, see, e.g., [12–24].

Some important quantities in axion physics, such as the axion mass and self-coupling, are dictated by the axion potential. The visible axion models [10, 11] with the axion decay constant at the electroweak scale or even smaller are believed to have been ruled out by experiments. For the invisible axion [25–28], its mass window is usually assumed in the range from about $10^{-6}\,\mathrm{eV}$ to $10^{-2}\,\mathrm{eV}$. According to constraints from astrophysical observations, the present bounds on the axion decay constant is $10^9\,\mathrm{GeV} \lesssim f_a \lesssim 10^{12}\,\mathrm{GeV}$ [29, 30] (we refer to refs. [24, 31–34] for several recent reviews).[1] Within the above available parameter space, the axion may be the main source of cold dark matter in the universe [36–41]. In addition, it may form a Bose-Einstein condensate [42] or even compact boson stars [43–49]. The axion can couple to the Standard Model (SM) particles like electrons, nucleons, photons and so on. However, all these couplings are suppressed by the axion decay constant f_a, which is remarkably large, resulting in the invisible axion which has very weak couplings to the SM particles [36]. Since the axion-photon coupling vertex, see eq. (4.1) below, allows for the production of an axion from the interaction of a photon with a background magnetic field, the axion-photon coupling $g_{a\gamma\gamma}$ plays a central role in axion searches in both laboratory experiments and stellar objects [24]. In this case it is very useful to study the axion properties, especially the axion-photon coupling, at a high precision from the theoretical point of view.

At low energies in QCD, all hadronic degrees of freedom are frozen and thus can be neglected except for the pseudo-Goldstone bosons of the spontaneous chiral symmetry breaking. Chiral perturbation theory (CHPT) [50–52], as the low-energy effective theory of QCD, can be used to describe the vacuum properties as well as the dynamics of QCD in the non-perturbative regime reliably. In this paper, we will calculate the θ-vacuum energy density, or equivalently the QCD axion potential, up-to-and-including next-to-leading order (NLO) in SU(N) CHPT. Setting $N = 3$, the mass and self-couplings of the axion can then be extracted from a Taylor expansion of the axion potential. In addition, we also compute the NLO corrections to the axion-photon coupling.

Before continuing, we would like to stress that a similar study was performed in ref. [53], where the QCD axion potential derived in two-flavor CHPT up to NLO (the QCD θ-vacuum energy density up to NLO was first derived in ref. [54]) is used, and a matching between two-flavor and three-flavor CHPT is performed to determine the axion-photon coupling. Here, the calculations are explicitly done in SU(N) CHPT for the θ-vacuum energy density and with $N = 3$ for the other quantities. In SU(3) CHPT, the topological susceptibility as well as the fourth cumulant of the topological distribution up to NLO have been calculated before using the Goldstone boson masses at $\theta = 0$ [55–57]. Very recently, the topological susceptibility and axion mass are calculated up to next-to-next-to-leading order and including electromagnetic corrections up to $\mathcal{O}(\alpha_{\mathrm{em}})$ in SU(2) CHPT [58]. The axion-nucleon coupling is also calculated up to the leading one-loop order in ref. [59]. Here, we derive the one-loop contribution to the SU(N) θ-vacuum energy density by a direct calculation of the logarithm of the functional determinant for the Goldstone bosons in a

[1] It was recently argued that there is still a possibility for a viable QCD axion model with a mass in the MeV range [35].

JHEP05(2020)001

θ-vacuum, extending the two-flavor treatment in ref. [54] to the case of N non-degenerate flavors.[2] This study is useful when the up and down quark masses take values close to the strange quark one. This could happen in lattice QCD calculations where the quark masses are parameters that can be chosen freely.

The outline of the paper is as follows. In section 2, we generalize the calculation of the θ-vacuum energy density in the framework of SU(2) CHPT [54] to the SU(N) case with N non-degenerate quark masses. In section 3, we derive the axion properties, including the mass and self-coupling, in detail for $N = 3$. In section 4, the model-independent part of the axion-photon coupling is determined from the chiral Lagrangian supplemented with the odd-intrinsic-parity sector of the chiral effective Lagrangian. Section 5 contains a brief summary and discussion. The appendix provides a relatively detailed derivation of the recursion relation giving rise to the general solution of the vacuum angles ϕ_f.

2 θ-vacuum energy density up to NLO

The QCD axion potential as a function of a/f_a has the same form as the QCD θ-vacuum energy density as a function of θ. In this section, we compute the θ-vacuum energy density in SU(N) CHPT with N non-degenerate quark masses, which is an extension of ref. [54], where the θ-vacuum energy is computed up to NLO in the SU(2) and SU(N)-symmetric cases.

2.1 Leading order

The discovery of instantons not only solved the U(1)$_A$ problem, but also implied that there is a θ-term in the QCD Lagrangian. In order to study the physics with a θ parameter, it is common to rotate away the θ-term by performing a chiral rotation on the quark fields. At low energies, we can then match the resulting Lagrangian to the chiral Lagrangian since now the relevant degrees of freedom are the pseudo-Goldstone bosons [51, 52]. The Lagrangian density of the SU(N) CHPT at leading order (LO) in a θ-vacuum is

$$\mathcal{L}^{(2)} = \frac{F_0^2}{4}\Big[\langle D_\mu U D^\mu U^\dagger\rangle + \langle \chi_\theta U^\dagger + U\chi_\theta^\dagger\rangle\Big], \tag{2.1}$$

where $\chi_\theta = 2B_0\mathcal{M}_q \exp[i\mathcal{X}_a\theta]$ contains the θ angle and the diagonal and real quark mass matrix is $\mathcal{M}_q = \mathrm{diag}\{m_1, m_2, \ldots, m_N\}$, and $\langle\ldots\rangle$ denotes the trace in the flavor space. The matrix $\mathcal{X}_a$ takes the following general form:

$$\mathcal{X}_a = \mathrm{diag}\{\mathcal{X}_1, \mathcal{X}_2, \ldots, \mathcal{X}_N\}, \quad \langle\mathcal{X}_a\rangle = 1, \tag{2.2}$$

which arises from a U(1)$_A$ chiral rotation on the quark fields eliminating the θ-term in the QCD Lagrangian. In this case, the θ-dependence is completely captured by the quark mass term. The U(1)$_A$ chiral rotation can be distributed to different quark flavors, leading to different choices of $\mathcal{X}_a$. F_0 is the pion decay constant in the three-flavor chiral limit, and $B_0 = -\langle\bar{q}q\rangle/F_0^2$ is related to the scalar quark condensate. U(x) is the field configuration for the vacuum and the Goldstone bosons of the spontaneous breaking of chiral symmetry.

[2] For an investigation of the axion interactions with mesons and photons using a 3-flavor chiral Lagrangian including the U(1)$_A$ anomaly, see ref. [60].

JHEP05(2020)001

It can be written as $\mathrm{U}(x) = U_0\tilde{U}(x)$, where $\tilde{U}(x)$ collects the Goldstone bosons, and U_0 describes the vacuum, parameterized as

$$U_0 = \mathrm{diag}\{e^{i\varphi_1}, e^{i\varphi_2}, \ldots, e^{i\varphi_N}\} \tag{2.3}$$

subject to the constraint $\sum_{i=1}^{N}\varphi_i = 0$ [55, 61]. For the SU(3) case, $\tilde{U} = e^{i\Phi/F_0}$, with Φ given by

$$\Phi = \begin{pmatrix} \pi_3 + \frac{1}{\sqrt{3}}\eta_8 & \sqrt{2}\pi^+ & \sqrt{2}K^+ \\ \sqrt{2}\pi^- & -\pi_3 + \frac{1}{\sqrt{3}}\eta_8 & \sqrt{2}K^0 \\ \sqrt{2}K^- & \sqrt{2}\bar{K}^0 & -\frac{2}{\sqrt{3}}\eta_8 \end{pmatrix}. \tag{2.4}$$

Note that the neutral flavor eigenstates in the octet of the pseudoscalar mesons as shown above, i.e. π_3 and η_8, are not mass eigenstates. Diagonalizing the mass matrix of the meson fields, one gets the physical mass eigenstates π^0 and η, which are mixtures of π_3 and η_8. By expanding the LO Lagrangian in terms of the meson fields to quadratic order, the LO θ-dependent meson masses including isospin breaking effects are obtained as

$$\begin{aligned}
\mathring{M}^2_{\pi^\pm} &= B_0(m_1\cos\phi_1 + m_2\cos\phi_2), \\
\mathring{M}^2_{K^\pm} &= B_0(m_1\cos\phi_1 + m_3\cos\phi_3), \\
\mathring{M}^2_{K^0} &= \mathring{M}^2_{\bar{K}^0} = B_0(m_2\cos\phi_2 + m_3\cos\phi_3), \\
\mathring{M}^2_{\pi^0} &= B_0(m_1\cos\phi_1 + m_2\cos\phi_2) - \xi, \\
\mathring{M}^2_{\eta} &= \frac{1}{3}B_0\left(m_1\cos\phi_1 + m_2\cos\phi_2 + 4m_3\cos\phi_3\right) + \xi\,,
\end{aligned} \tag{2.5}$$

where for convenience we have defined $(m_1, m_2, m_3) \equiv (m_u, m_d, m_s)$ and

$$\phi_f \equiv \mathcal{X}_f\theta - \varphi_f. \tag{2.6}$$

The parameter ξ is given by

$$\xi = \frac{4}{3}B_0\left(m_3\cos\phi_3 - \frac{1}{2}(m_1\cos\phi_1 + m_2\cos\phi_2)\right)\frac{\sin^2\epsilon_\theta}{\cos(2\epsilon_\theta)} = \mathcal{O}\left(\epsilon_\theta^2\right), \tag{2.7}$$

with ϵ_θ the π^0-η mixing angle in the θ-vacuum, which arises due to strong isospin breaking. Diagonalization of the mass matrix requires

$$\tan 2\epsilon_\theta = \frac{\sqrt{3}(m_2\cos\phi_2 - m_1\cos\phi_1)}{2m_3\cos\phi_3 - m_1\cos\phi_1 - m_2\cos\phi_2}\,. \tag{2.8}$$

Obviously, the above θ-dependent Goldstone boson masses reduce to the standard SU(3) relations [52] by taking the limit $\theta = 0$ and setting $\phi_f = 0$. The dependence of ϕ_f on the θ angle needs to be determined by minimizing the vacuum energy to be discussed below.

To determine the ground state, i.e. the vacuum, we set $\tilde{U} = \mathbb{1}$. Performing the trace in eq. (2.1), one obtains the LO potential energy density

$$e^{(2)}_{\mathrm{vac}} = -F_0^2B_0\sum_f m_f\cos\phi_f. \tag{2.9}$$

JHEP05(2020)001

Moreover, minimizing eq. (2.9) with respect to the parameters ϕ_f with the constraint $\sum_f \phi_f = \theta$ gives the following equations[3]

$$\begin{cases} m_1 \sin\phi_1 = m_2 \sin\phi_2 = m_3 \sin\phi_3, \\ \sum_f \phi_f = \theta, \end{cases} \tag{2.10}$$

for SU(3), and similar equations for SU(N), i.e., $m_f \sin\phi_f$ is the same for all flavors. The above equations depend only on the linear combination ϕ_f given in eq. (2.6), instead of on $\mathcal{X}_f$ and φ_f separately. This implies that ϕ_f is physical while $\mathcal{X}_f$ and φ_f are not. One can use this freedom to choose the "gauge" most convenient for the question of interest. One possible choice is to choose $\mathcal{X}_a = \mathbb{1}/N$, which is commonly used in the literature (see, e.g., refs. [54, 55, 61–63]). Noticing that the only constraint on $\mathcal{X}_a$ is $\langle \mathcal{X}_a \rangle = 1$, one may also choose the U(1)$_A$ rotations to be

$$\mathcal{X}_f = \frac{\phi_f}{\theta}, \quad \text{and} \quad \varphi_f = 0 \tag{2.11}$$

to simultaneously shift the θ angle to the quark mass matrix phase and align the vacuum properly. This is a convenient choice for the $a\gamma\gamma$ coupling (with θ changed to the dynamical axion field a/f_a) to be discussed in section 4 since this removes the leading order a-π^0 and a-η mixing.

The equations (2.10) do not admit an analytical solution in terms of elementary functions in a compact form.[4] In the isospin symmetric case, the up and down quark masses are degenerate $m_1 = m_2 \equiv m$ but $m \neq m_3$, we have $\phi_1 = \phi_2 \equiv \phi$, and then eq. (2.10) becomes [64]

$$m \sin\phi = m_3 \sin(\theta - 2\phi), \tag{2.12}$$

which allows for analytic solutions, though complicated ones.

If one focuses on the cumulants of the QCD topological distribution, which are derivatives of the vacuum energy density, $e_{\text{vac}}(\theta)$, with respect to θ,

$$c_{2n} = \left. \frac{d^{2n} e_{\text{vac}}(\theta)}{d\theta^{2n}} \right|_{\theta=0}, \quad n \in \mathbb{N}, \tag{2.13}$$

one may solve eqs. (2.10) by expanding in powers of θ. Specifically, c_2 corresponds to the topological susceptibility. Up to $\mathcal{O}\left(\theta^3\right)$, one gets [55]

$$\phi_f = \frac{\bar{m}}{m_f}\theta + \left[\left(\frac{\bar{m}}{m_f} \right)^3 - \frac{\bar{m}^4}{m_f \bar{m}^{[3]}} \right] \frac{\theta^3}{6} + \mathcal{O}(\theta^5), \tag{2.14}$$

where we have introduced

$$\frac{1}{\bar{m}} = \sum_i \frac{1}{m_i}, \quad \frac{1}{\bar{m}^{[3]}} = \sum_i \frac{1}{m_i^3} \tag{2.15}$$

[3] For the vacuum alignment in SU(2) CHPT up to NLO, we refer to the appendix of ref. [62], which also shows that it is sufficient to consider the LO vacuum alignment for the computation of the cumulants up to $\mathcal{O}\left(p^4\right)$.

[4] In the SU(2) case, there is an analytic solution [61], which then allows to derive a closed form of the vacuum energy density up to NLO in the chiral expansion [54].

JHEP05(2020)001

with i running over all the flavor indices considered in the theory. The solutions in eq. (2.14) are not restricted to the three-flavor case but also valid for $N > 3$. Consequently, the θ-dependence of the vacuum energy density at LO can be obtained by substituting the solution in eq. (2.14) into eq. (2.9), which gives [55]

$$e_{\rm vac}^{(2)}(\theta) = F_0^2 B_0 \left(\frac{1}{2}\bar{m}\theta^2 - \frac{\bar{m}^4}{24\bar{m}^{[3]}}\theta^4 \right) + \mathcal{O}(\theta^6). \tag{2.16}$$

In appendix A, we work out a recursion relation for ϕ_f up to an arbitrary power of θ,

$$\phi_f = \sum_{n=0}^{\infty} C_{f,2n+1}\theta^{2n+1}, \tag{2.17}$$

with $C_{f,1} = \bar{m}/m_f$ and

$$C_{f,2n+1} = \sum_{t=1}^{n} \sum_{(k_1,\ldots,k_t)} s_{K_t} \binom{K_t}{k_1,\ldots,k_t} \left[\frac{\bar{m}}{m_f} \sum_{i=1}^{N} \prod_{j=1}^{t} C_{i,2j-1}^{k_j} - \prod_{j=1}^{t} C_{f,2j-1}^{k_j} \right], \tag{2.18}$$

where k_j are non-negative integers, $K_t \equiv \sum_{j=1}^{t} k_j$, $\sum_{(k_1,\ldots,k_t)}$ means that the sum runs over all possibilities of k_j satisfying $k_1 + \cdots + (2t-1)k_t = 2n+1$, $s_{K_t} = (-1)^{(K_t-1)/2}/(K_t!)$, and $\binom{K_t}{k_1,\ldots,k_t} = K_t!/(k_1!\cdots k_t!)$ are the multinomial coefficients.

In the next subsection, we will compute the one-loop contribution of the Goldstone bosons to the energy density.

2.2 Next-to-leading order

To study the θ-vacuum energy up to the NLO, $\mathcal{O}(p^4)$, one has to include both the tree-level diagrams from $\mathcal{L}^{(4)}$ and the one-loop diagrams with innsertions from $\mathcal{L}^{(2)}$. The SU(N) chiral Lagrangian at NLO is given by

$$\mathcal{L}^{(4)} = L_6\langle\chi_\theta U^\dagger + U\chi_\theta^\dagger\rangle^2 + L_7\langle\chi_\theta U^\dagger - U\chi_\theta^\dagger\rangle^2 + L_8\langle\chi_\theta^\dagger U\chi_\theta^\dagger U + U^\dagger\chi_\theta U^\dagger\chi_\theta\rangle + H_2\langle\chi_\theta^\dagger\chi_\theta\rangle, \tag{2.19}$$

where we only display the terms relevant for the vacuum energy. The L_i and H_2 are the so-called low-energy constants (LECs) and the high-energy constant (HEC), respectively. The latter is only required for renormalization and does not appear in observables. After setting $U = U_0$ and evaluating the traces, one gets the tree-level contribution to the NLO vacuum energy density

$$e_{\rm vac}^{(4,\rm tree)} = -16B_0^2 \left[L_6 \left(\sum_i m_i \cos\phi_i \right)^2 - L_7 \left(\sum_i m_i \sin\phi_i \right)^2 + \frac{L_8}{2} \sum_i m_i^2 \cos(2\phi_i) + \frac{H_2}{4} \sum_i m_i^2 \right]. \tag{2.20}$$

The LECs and HEC contain both ultraviolet (UV) finite and divergent parts. They are related to the renormalized ones, denoted by an upper index r, by [52, 65]

$$L_6 = L_6^r + \frac{N^2+2}{16N^2}\lambda, \quad L_8 = L_8^r + \frac{N^2-4}{16N}\lambda, \quad L_7 = L_7^r, \quad H_2 = H_2^r + \frac{N^2-4}{8N}\lambda, \tag{2.21}$$

JHEP05(2020)001

with

$$\lambda = \frac{\mu^{d-4}}{16\pi^2}\left\{\frac{1}{d-4} - \frac{1}{2}\left[\ln(4\pi) + \Gamma'(1) + 1\right]\right\} \tag{2.22}$$

the UV divergence at the space-time dimension $d = 4$, where μ is the scale of dimensional regularization. The UV divergence in the NLO tree-level contribution exactly cancels the one arising in the one-loop contribution, as will be seen below.

Now let us calculate the one-loop contribution to the θ-vacuum energy density. In the classical CHPT papers [51, 52], the one-loop effective generating functional is expanded around the free-field configuration at $\theta = 0$. This treatment is then applied to derive the topological susceptibility and the fourth cumulant in SU(N) CHPT in refs. [55, 56, 63]. The expression for the vacuum energy density at NLO in SU(2) with non-degenerate quark masses, as well as that in SU(N) with degenerate quark masses, is derived in ref. [54], where the generating functional is expanded around the free-field configuration in the θ-vacuum. The result allows for an evaluation of any cumulant of the QCD topological charge distribution, and is the QCD axion potential at NLO [53]. Here, we generalize the result in ref. [54] to SU(N), with N non-degenerate quark masses. The effective action for the free-field configuration in the θ-vacuum is

$$Z_0(\theta) = \frac{i}{2}\ln\det D_0(\theta) = \frac{i}{2}\mathrm{Tr}\ln D_0(\theta), \tag{2.23}$$

where "Tr" denotes traces over both the flavor (in the adjoint representation) and the coordinate spaces, and the differential operator $D_0(\theta)$ takes the following form

$$D_{0,PY}(\theta) = \delta_{PY}\left[\partial^\mu\partial_\mu + \mathring{M}_P^2(\theta)\right], \tag{2.24}$$

where $P, Y = 1, \ldots, N^2 - 1$ are the flavor indices of the Goldstone bosons, and $\mathring{M}_P(\theta)$ are θ-dependent meson masses at LO given in eq. (2.5). Within dimensional regularization, one gets the one-loop contribution to the vacuum energy density as [54]

$$\begin{aligned} e_{\mathrm{vac}}^{(4,\mathrm{loop})} &= -\frac{Z_0(\theta)}{V} \\ &= -\frac{i}{2}\sum_P \int \frac{d^dp}{(2\pi)^d}\ln\left[-p^2 + \mathring{M}_P^2(\theta)\right] \\ &= \sum_P \mathring{M}_P^4(\theta)\left\{\frac{\lambda}{2} - \frac{1}{128\pi^2}\left[1 - 2\ln\frac{\mathring{M}_P^2(\theta)}{\mu^2}\right]\right\}, \end{aligned} \tag{2.25}$$

where V is the space-time volume, the P runs over the Goldstone boson mass eigenstates (for the SU(3) case, they are given in eq. (2.5)), and the term proportional to λ collects all the UV divergences in the one-loop contribution.

Noticing that the matrix elements of the diagonalized mass-squared matrix of the Goldstone bosons are given by

$$\delta_{PY}\mathring{M}_P^2(\theta) = \frac{1}{8}\left\langle\left\{\lambda_P, \lambda_Y^\dagger\right\}\left(\chi_\theta^\dagger U_0 + U_0^\dagger\chi_\theta\right)\right\rangle \equiv \sigma_{PY}, \tag{2.26}$$

JHEP05(2020)001

we obtain

$$\sum_P \mathring{M}_P^2(\theta) = \sum_P \sigma_{PP} = \frac{2(N^2-1)}{N} \sum_i m_i \cos\phi_i. \tag{2.27}$$

Similarly, we have

$$\begin{aligned}\sum_P \mathring{M}_P^4(\theta) &= \sum_{P,Y} \sigma_{PY}\sigma_{YP} \\ &= 2B_0^2 \left[\frac{N^2+2}{N^2} \left(\sum_i m_i \cos\phi_i \right)^2 + \frac{N^2-4}{N} \sum_i (m_i \cos\phi_i)^2 \right]. \end{aligned} \tag{2.28}$$

With eqs. (2.20), (2.21), (2.25) and (2.28), it is straightforward to check that the UV divergence in the one-loop contribution exactly cancels that in the tree-level contribution. Finally, we obtain the θ-vacuum energy density up to NLO as

$$\begin{aligned} e_{\rm vac} = &-F_0^2 B_0 \sum_i m_i \cos\phi_i - \sum_P \frac{\mathring{M}_P^4(\theta)}{128\pi^2} \left[1 - 2\ln \frac{\mathring{M}_P^2(\theta)}{\mu^2} \right] \\ &- 16 B_0^2 \left[L_6^r \left(\sum_i m_i \cos\phi_i \right)^2 + N \left(N L_7^r + L_8^r \right) m_1^2 \cos^2\phi_1 \right], \end{aligned} \tag{2.29}$$

where we have used the SU(N) version of eq. (2.10) to replace all $m_i \sin\phi_i$ by $m_1 \sin\phi_1$, and have neglected the θ-independent terms.

From the above θ-vacuum energy density, the lowest two cumulants of the topological charge distribution up to NLO can then be easily extracted. It can be checked from eq. (2.29) that we can reproduce the expression of topological susceptibility at NLO keeping all orders in strong isospin breaking exactly given in ref. [66]. We are more interested in the axion mass and its self-coupling, and thus we will extract them from the axion potential based on the relation between the θ-vacuum energy and axion potential in the following section. Numerical values of the topological susceptibility and the normalized fourth cumulant will also be given for reference.

3 Axion mass and self-coupling

Both the axion mass and self-coupling are important quantities, since they directly affect experimental searches for the axion. For example, one tries to detect the axion in microwave cavities by stimulating their conversion to photons via the Primakoff effect within an external magnetic field [24]. The axion self-coupling plays an important role in the formation of an axion Bose-Einstein condensation [42] as well as possible boson stars [43–45, 47, 67]. This motivates the study of these two quantities in this section to high precision. Before we proceed to derive the axion mass and self-coupling up to NLO, let us discuss a little bit about the axion solution to the strong CP problem, and start with the effective Lagrangian,

$$\mathcal{L}_{G\tilde{G}} = \left(\theta + \frac{a}{f_a} \right) \frac{g_s^2}{32\pi^2} G^c_{\mu\nu} \tilde{G}^{c,\mu\nu}, \tag{3.1}$$

JHEP05(2020)001

where in addition to the θ-term, a pseudoscalar axion field is introduced which couples to gluons. As shown by Peccei and Quinn [8, 9], the periodicity of the vacuum expectation value (VEV) $\langle G\tilde{G}\rangle$ in $\theta+a/f_a$ forces the minimum of the axion VEV to be at $\theta+\langle a\rangle/f_a = 0$, and thus the θ-dependence is eliminated. Expanding the axion field around its VEV, one sees that the θ-vacuum energy density derived in the previous section, with θ being replaced by $a_{\rm phys}/f_a$, gives the axion potential, where $a_{\rm phys} = a - \langle a\rangle$ is the physical axion field. In the following we will denote $a_{\rm phys}$ as a for simplicity, and then the axion potential is given by $V(a) = e_{\rm vac}(a/f_a)$.

Expanding $V(a)$ in powers of the axion field around the vacuum, we obtain

$$V(a) = \frac{1}{2}m_a^2 a^2 + \sum_{n=2}^{\infty}\frac{1}{(2n)!}\lambda_{2n}a^{2n}\,. \tag{3.2}$$

Comparing the above equation with the definition of cumulants of the QCD topological distribution in eq. (2.13), one finds the following relations for the axion mass and axion self couplings:

$$m_a^2 = \frac{c_2}{f_a^2}, \quad \lambda_{2n} = \frac{c_{2n}}{f_a^{2n}}\,, \tag{3.3}$$

where c_{2n} are the cumulants defined in eq. (2.13) with $n \geq 2$. Thus, the axion mass and four-axion self-coupling at LO are given by

$$m_{a,\rm LO}^2 = \frac{F_\pi^2 M_{\pi^+}^2 \bar{m}}{2f_a^2\hat{m}}, \quad \lambda_{4,\rm LO} = -\frac{F_\pi^2 M_{\pi^+}^2 \bar{m}^4}{2f_a^4 \bar{m}^{[3]}\hat{m}}, \tag{3.4}$$

respectively, where $\hat{m} = (m_u + m_d)/2$, and we have replaced B_0 and F_0 by $M_{\pi^+}^2/(2\hat{m})$ and F_π, the physical pion mass squared and decay constant, respectively, which is legitimate at LO. One sees that at LO, the difference between the SU(3) and SU(2) expressions resides merely in the definitions of $\bar{m}$ and $\bar{m}^{[3]}$ in eq. (2.15).

In the same way we have calculated the axion mass and self-couplings at LO. Their expressions at NLO, including the higher order corrections, can be extracted from eq. (2.29). The former reads

$$\begin{aligned} m_a^2 = \frac{F_\pi^2 M_{\pi^+}^2 \bar{m}}{2f_a^2\hat{m}}\Bigg\{1 + \frac{16M_{\pi^+}^2}{F_\pi^2}\left[\frac{3\bar{m}}{\hat{m}}(3L_7^r + L_8^r) - L_8^r\right] \\ + \frac{\bar{m}}{m_s}\left(\mu_{\pi^0} + 2\mu_{\pi^+} - \mu_\eta\right) + \left(2\frac{\bar{m}}{m_d} - 1\right)\mu_{K^+} + \left(2\frac{\bar{m}}{m_u} - 1\right)\mu_{K^0} + \mathcal{O}\left(\frac{\delta^2}{m_s^2}\right)\Bigg\}, \end{aligned} \tag{3.5}$$

with $\mu_P = \frac{M_P^2}{32\pi^2 F_\pi^2}\ln\frac{M_P^2}{\mu^2}$ and $\delta = m_d - m_u$, where we have used the NLO expressions for the pion mass and decay constant [52]:

$$\begin{aligned} M_{\pi^+}^2 &= B_0(m_u + m_d)\left\{1 + \mu_{\pi^0} - \frac{1}{3}\mu_\eta + \frac{16B_0}{F_0^2}\left[\hat{m}\left(2L_8^r - L_5^r\right) + (2\hat{m} + m_s)\left(2L_6^r - L_4^r\right)\right]\right\}, \\ F_\pi &= F_0\left\{1 - \mu_{\pi^+} - \mu_{\pi^0} - \frac{\mu_{K^+}}{2} - \frac{\mu_{K^0}}{2} + \frac{8B_0}{F_0^2}\left[\hat{m}L_5^r + (2\hat{m} + m_s)L_4^r\right]\right\}. \end{aligned} \tag{3.6}$$

JHEP05(2020)001

Similarly the self-coupling up to NLO can be easily obtained as

$$\begin{aligned}\lambda_4 = &-\frac{F_\pi^2 M_{\pi^+}^2 \bar{m}^4}{2 f_a^4 \hat{m} \bar{m}^{[3]}} \Bigg\{ 1 + \frac{16 M_{\pi^+}^2}{F_\pi^2} \left[\frac{3\bar{m}^{[3]}}{\hat{m}\bar{m}^2} L_6^r + 36 \frac{\bar{m}}{\hat{m}} L_7^r + \left(12 \frac{\bar{m}}{\hat{m}} - 1 \right) L_8^r \right] \\ &+ \left[\frac{3\bar{m}^{[3]}}{m_u^3} \left(1 - \frac{m_u}{m_d} \right)^2 \left(1 + \frac{m_u}{m_d} \right) + \frac{4\bar{m}}{m_s} - 3 \right] \left(\mu_{\pi^0} + 2\mu_{\pi^+} \right) \\ &+ \left[\frac{6\bar{m}^{[3]}}{m_s^3} \left(1 - \frac{m_s}{m_d} \right)^2 \left(1 + \frac{m_s}{m_d} \right) + \frac{8\bar{m}}{m_u} - 7 \right] \mu_{K^0} \\ &+ \left[\frac{6\bar{m}^{[3]}}{m_s^3} \left(1 - \frac{m_s}{m_u} \right)^2 \left(1 + \frac{m_s}{m_u} \right) + \frac{8\bar{m}}{m_d} - 7 \right] \mu_{K^+} \\ &+ \left[\frac{3\bar{m}^{[3]}}{m_s^3} - \frac{4\bar{m}}{m_s} - \frac{\bar{m}^{[3]} (m_s + 3\bar{m})^2}{m_s^2 \bar{m}^2 (m_u + m_d + 4m_s)} \right] \mu_\eta + \mathcal{O}\left(\frac{\delta^2}{m_s^2} \right) \Bigg\} \\ &+ \frac{3\bar{m}^4}{32\pi^2 f_a^4} \left[\frac{3M_{\pi^+}^4}{m_u^2 m_d^2} + \frac{2M_{K^+}^4}{m_u^2 m_s^2} + \frac{2M_{K^0}^4}{m_d^2 m_s^2} + \frac{\left(2m_u M_{K^0}^2 + 2m_d M_{K^+}^2 - m_s M_{\pi^+}^2 \right)^2}{9 m_u^2 m_d^2 m_s^2} \right]. \end{aligned} \tag{3.7}$$

The numerical evaluation requires the values of the quark mass ratios and of the LECs, which have been determined by the lattice QCD calculations and experimental data. A review of the present knowledge of the LECs appearing in the chiral Lagrangian for the meson sector can be found in ref. [68]. Using the input values listed in table 1, we find the axion mass and the quartic axion self-coupling at NLO to be

$$m_a = 5.89(10)\mu\text{eV} \cdot \frac{10^{12}\ \text{GeV}}{f_a}\,, \tag{3.8}$$

$$\lambda_4 = -\left(5.86(19) \cdot \frac{10^{-2}\,\text{GeV}}{f_a} \right)^4\,, \tag{3.9}$$

respectively. Here we have used the charged pion mass in eq. (3.6) for eliminating the overall $B_0(m_u+m_d)$ factor in m_a^2 and λ_4. Although the difference between the charged and neutral pions from QCD is of $\mathcal{O}\left(\delta^2\right)$, the charged pion receives an electromagnetic contribution at LO. Such an effect to the quantities of interest here can be eliminated if using the neutral pion mass instead, which amounts to replacing $M_{\pi^+}^2$ by $M_{\pi^0}^2$ in eqs. (3.5) and (3.7) and adding the following terms inside the curly brackets of these two expressions [52]:

$$\frac{\left(M_{K^+}^2 - M_{K^0}^2 \right)_{\text{QCD}}^2}{3M_{\pi^0}^2 \left(M_\eta^2 - M_{\pi^0}^2 \right)} \left[1 + \frac{8}{3}\Delta_{\text{GMO}} + \frac{M_{K^0}^2}{8\pi^2 F_\pi^2} \left(1 + 6 \ln \frac{M_{K^0}^2}{M_\eta^2} \right) + \mathcal{O}\left(\hat{m}, m_s \right) \right], \tag{3.10}$$

with

$$\begin{aligned} \left(M_{K^+}^2 - M_{K^0}^2 \right)_{\text{QCD}} &= M_{K^0}^2 - M_{K^+}^2 - M_{\pi^0}^2 + M_{\pi^+}^2\,, \\ \Delta_{\text{GMO}} &= \frac{2M_{K^0}^2 + 2M_{K^+}^2 - 2M_{\pi^+}^2 + M_{\pi^0}^2 - 3M_\eta^2}{M_\eta^2 - M_{\pi^0}^2}, \end{aligned} \tag{3.11}$$

JHEP05(2020)001

z	r	M_{π^+}	M_{π^0}	M_{K^+}	M_{K^0}	M_η
0.485(19)	27.42(12)	139.57	134.98	493.68(2)	497.61(1)	547.86(2)
F_π	L_6^r	L_7^r	L_8^r	C_7^W	C_8^W	
92.28(9)	0.0(4)	$-0.3(2)$	0.5(2)	≈ 0	0.60 ± 0.20	

Table 1. Numerical inputs used in this paper. The pion decay constant F_π, and experimental meson masses M_P are in units of MeV, and are taken from ref. [33]. The renormalized LECs L_i^r are in units of 10^{-3}; they correspond to values at scale $\mu = 770\,\text{MeV}$ and are taken from ref. [68]. The NNLO anomalous LECs C_7^W and C_8^W are given in units of $10^{-3}\,\text{GeV}^{-2}$; for their determinations, see the text. For the quark mass ratios defined as $z = m_u/m_d$ and $r = m_s/\hat{m}$, we take the FLAG average of the $N_f = 2+1$ lattice results [70].

where the electromagnetic effects have been taken into account. As a result, the values in eqs. (3.8) and (3.9) become

$$m_a = 5.71(9)\mu\text{eV} \cdot \frac{10^{12}\ \text{GeV}}{f_a}\,, \tag{3.12}$$

$$\lambda_4 = -\left(5.77(18) \cdot \frac{10^{-2}\,\text{GeV}}{f_a}\right)^4\,, \tag{3.13}$$

which are regarded as our results for these quantities and will be used in the following.

As we mentioned earlier, both the axion mass and its self-coupling are tightly related to the cumulants of the QCD topological charge distribution through the θ-vacuum energy density, see eq. (3.3). Thus, from eq. (2.13) or (3.3) we can further extract the numerical values of the topological susceptibility χ_t and the normalized fourth cumulant $b_2 = c_4/(12\chi_t)$ [56] with the inclusion of isospin breaking effects at zero temperature, i.e.,

$$\chi_t^{1/4} = \sqrt{m_a f_a} = 75.6(6)\,\text{MeV}\,, \tag{3.14}$$

$$b_2 = \frac{\lambda_4 f_a^2}{12 m_a^2} = -0.028(3)\,. \tag{3.15}$$

Since the masses of the octet of pseudoscalar mesons are well-known from experiments, the uncertainties are in fact dominated by the renormalized LEC L_7^r, while the subdominant uncertainties are from the quark mass ratio $z = m_u/m_d$ and the LECs L_6^r and L_8^r. In comparison, the values of these quantities obtained here remain almost the same as the one in SU(2) case numerically, which are $\chi_t^{1/4} = 75.5(5)\,\text{MeV}$ and $b_2 = -0.029(2)$ [53]. And the result for the topological susceptibility is in perfect agreement with recent $N_f = 2+1+1$ lattice QCD simulation at the physical point giving $\chi_t^{1/4} = 75.6(1.8)(0.9)\,\text{MeV}$ [69]. This indicates that the explicit inclusion of the strange quark degree of freedom does not induce large differences on the axion properties. There are at least two compelling reasons accounting for this feature. First, the effects from the heavier quark flavors have been largely included in the corresponding SU(2) LECs. Second, in ref. [53] the authors performed their numerical calculations with a matching between two-flavor and three-flavor CHPT LECs. Thus, the inclusion of the strange-quark degree of freedom does not change the results

JHEP05(2020)001

sizeably. Yet, the expressions given here should be useful for chiral extrapolation of lattice results performed at unphysical quark masses, in particular when the up and down quark masses are close to the strange quark one.

4 Axion-photon coupling

The axion-photon coupling is defined by the following Lagrangian (see, e.g., refs. [53,71,72]),

$$\mathcal{L}_{a\gamma\gamma} = \frac{1}{4} g_{a\gamma\gamma} a F^{\mu\nu} \tilde{F}_{\mu\nu}, \tag{4.1}$$

where $\tilde{F}_{\mu\nu} = \frac{1}{2}\varepsilon_{\mu\nu\rho\sigma}F^{\rho\sigma}$, with $F^{\mu\nu}$ the electromagnetic field tensor with the sign convention $\epsilon_{0123} = +1$. Specifically, the axion-photon coupling is given by

$$\begin{aligned} g_{a\gamma\gamma} &= \frac{\alpha_{\rm em}}{2\pi f_a}\frac{\mathcal{E}}{\mathcal{C}} + g^{\rm QCD}_{a\gamma\gamma}, \\ g^{\rm QCD}_{a\gamma\gamma} &= -\frac{\alpha_{\rm em}}{2\pi f_a} 6\langle \mathcal{X}_a Q^2\rangle + g^{\rm mix}_{a\gamma\gamma} = -\frac{\alpha_{\rm em}}{2\pi f_a}\left(\frac{2}{3} + 2\mathcal{X}_u\right) + g^{\rm mix}_{a\gamma\gamma}, \end{aligned} \tag{4.2}$$

where $\mathcal{E}/\mathcal{C}$ is the ratio of the electromagnetic and color anomaly coefficients, which is given by $\sum_n (Q_{\rm PQ}Q^2)/\sum_n (Q_{\rm PQ}T^2)$, with the sums running over all fermions with PQ charges $Q_{\rm PQ}$, and T^a the QCD color generators satisfying $\langle T^a T^b\rangle = T^2\delta^{ab}/2$. The value of $\mathcal{E}/\mathcal{C}$ depends on the specific axion models. The first term in $g^{\rm QCD}_{a\gamma\gamma}$ is the contribution from the axial rotation of the quark fields, $q \to \exp\left(i\frac{a}{2f_a}\mathcal{X}_a\gamma_5\right) q$ with $\langle \mathcal{X}_a\rangle = 1$ (here we use the convention $\gamma^5 = i\gamma^0\gamma^1\gamma^2\gamma^3$), which was introduced to eliminate the term $\frac{a}{f_a}\frac{\alpha_s}{8\pi}G^c_{\mu\nu}\tilde{G}^{c,\mu\nu}$ from the axion Lagrangian. The second term in $g^{\rm QCD}_{a\gamma\gamma}$, $g^{\rm mix}_{a\gamma\gamma}$, is the contribution from the a-π^0 and a-η mixings, with the π^0 and η coupled to two photons.

As discussed below eq. (2.10), there is a freedom of choosing the diagonal matrix $\mathcal{X}_a$ satisfying $\langle \mathcal{X}_a\rangle = 1$. If it is chosen as $\mathcal{X}_a = {\rm diag}\{\bar{m}/m_u, \bar{m}/m_d, \bar{m}/m_s\} = \bar{m}\mathcal{M}_q^{-1}$ as in refs. [29, 73], then $U = \tilde{U} = e^{i\Phi/F_0}$, see eq. (2.11), and there is no a-π^0 or a-η mixing term in the LO chiral Lagrangian. One obtains the $\mathcal{O}\left(p^4\right)$ contribution to the model-independent $a\gamma\gamma$ coupling to be

$$g^{{\rm QCD},(4)}_{a\gamma\gamma} = -\frac{\alpha_{\rm em}}{2\pi f_a}\frac{2\left(m_u + 3\bar{m}\right)}{3m_u}. \tag{4.3}$$

This result recovers the one derived in SU(2) CHPT [53] at $\mathcal{O}(p^4)$ in the limit of $m_s \to \infty$.

The same result can also be obtained by using other choices of $\mathcal{X}_a$. In that case, one needs to consider a-meson mixing. The Wess-Zumino-Witten (WZW) Lagrangian [74, 75] with an external photon field can be used to get the mixing contribution. The Lagrangian is given by [76–78]

$$\begin{aligned} \mathcal{L}^{\rm em}_{\rm WZW} =& -\frac{eN_c}{48\pi^2}\varepsilon^{\mu\nu\rho\sigma}A_\mu\left\langle Q\partial_\nu UU^\dagger\partial_\rho UU^\dagger\partial_\sigma UU^\dagger + QU^\dagger\partial_\nu UU^\dagger\partial_\rho UU^\dagger\partial_\sigma U\right\rangle \\ &+ i\frac{e^2N_c}{48\pi^2}\varepsilon^{\mu\nu\rho\sigma}\partial_\nu A_\rho A_\sigma\left\langle 2Q^2(U\partial_\mu U^\dagger - U^\dagger\partial_\mu U) - QU^\dagger Q\partial_\mu U + QUQ\partial_\mu U^\dagger\right\rangle, \end{aligned} \tag{4.4}$$

where $e > 0$ is the electric charge unit, Q and N_c denote the usual diagonal quark charge matrix, $Q = {\rm diag}\{2/3, -1/3, -1/3\}$ for the three-flavor case, and the number of quark

colors, respectively. Here the convention is such that U transforms under $\mathrm{SU}(3)_L \times \mathrm{SU}(3)_R$ as $U \to g_R U g_L^\dagger$ with g_L and g_R elements in $\mathrm{SU}(3)_L$ and $\mathrm{SU}(3)_R$, respectively. According to Weinberg's power counting scheme, the above WZW Lagrangian starts to contribute from $\mathcal{O}(p^4)$. The axion-meson mixing contribution can be obtained by substituting U in the above Lagrangian by $\exp\left(-i\mathcal{Y}_a \frac{a}{f_a}\right)$ with $\mathcal{Y}_a = \mathcal{X}_a - \bar{m}\mathcal{M}_q^{-1}$. One finds

$$g_{a\gamma\gamma}^{\mathrm{mix}} = \frac{\alpha_{\mathrm{em}}}{2\pi f_a}\left(2\mathcal{X}_u - 2\frac{\bar{m}}{m_u}\right). \tag{4.5}$$

Using eq. (4.2), one again gets the expression given in eq. (4.3).

Our goal in this section is to compute the axion-photon coupling to $\mathcal{O}(p^6)$. The chiral Lagrangian with a minimal set of terms in the anomalous-parity strong sector at $\mathcal{O}(p^6)$ has been given in ref. [79], not only for SU(2) but also for SU(N) with $N \geq 3$. Based on the anomalous Lagrangians, several works have been done in the anomalous-parity sector [80, 81]. In this work, only the terms proportional to C_7^W and C_8^W are relevant to the axion-photon coupling, which read

$$\mathcal{L}_{\mathrm{ano}}^{(6)} = iC_7^W \varepsilon^{\mu\nu\rho\sigma} \langle \chi_- f_{+\mu\nu} f_{+\rho\sigma} \rangle + iC_8^W \varepsilon^{\mu\nu\rho\sigma} \langle \chi_- \rangle \langle f_{+\mu\nu} f_{+\rho\sigma} \rangle \,, \tag{4.6}$$

where C_7^W and C_8^W are two LECs. We have taken the same notation as in ref. [79].

In the following, we choose $\mathcal{X}_f = \bar{m}/m_f$ and $U = \tilde{U}$ for the computation of the $a\gamma\gamma$ coupling. With this convention the diagrams relevant for the computation of the $\mathcal{O}(p^6)$ corrections to $g_{a\gamma\gamma}$ are depicted in figure 1: (a) the axion-pion and axion-eta mass mixing from the NLO tree-level Lagrangian; (b) the tree-level diagram from $\mathcal{L}_{\mathrm{ano}}^{(6)}$; (c) one-loop diagrams with one vertex taken from $\mathcal{L}_{\mathrm{WZW}}$ and the other one taken from the LO chiral Lagrangian; the contributions from diagrams (d) and (e) exactly cancel with each other with the upper photon line in diagram (d) being on shell. It is interesting to note that for the anomalous processes such as π^0, η and η' decaying into two photons, the one-loop contributions vanish when the up-down quark mass difference is neglected [82, 83]. Likewise, in the SU(2) case the sum of all one loop corrections vanishes when both photons in the final state are on-shell [53]. However, in the SU(3) case, diagram (c) does contribute to the axion-photon coupling at $\mathcal{O}(p^6)$ when taking isospin breaking effects into account. Note that the pion-eta mixing needs to be considered in order to keep $g_{a\gamma\gamma}$ scale-independent and UV finite.

Putting together all the pieces, we obtain the axion-photon coupling keeping all orders in strong isospin breaking up to $\mathcal{O}(p^6)$ as

$$\begin{aligned} g_{a\gamma\gamma} = \frac{\alpha_{\mathrm{em}}}{2\pi f_a}\Bigg\{ & \frac{\mathcal{E}}{\mathcal{C}} - \frac{2}{3}\frac{m_u + 3\bar{m}}{m_u} \\ & - \frac{1024\pi^2}{3\hat{m}}\bar{m}M_{\pi^0}^2\left(C_7^W + 3C_8^W\right) + \frac{2\bar{m}M_{\pi^0}^2}{3\hat{m}}\left[\frac{f_+(\cos,\sin)}{\sqrt{3}M_\eta^2} + \frac{f_-(\sin,\cos)}{M_{\pi^0}^2}\right]\Bigg\}, \end{aligned} \tag{4.7}$$

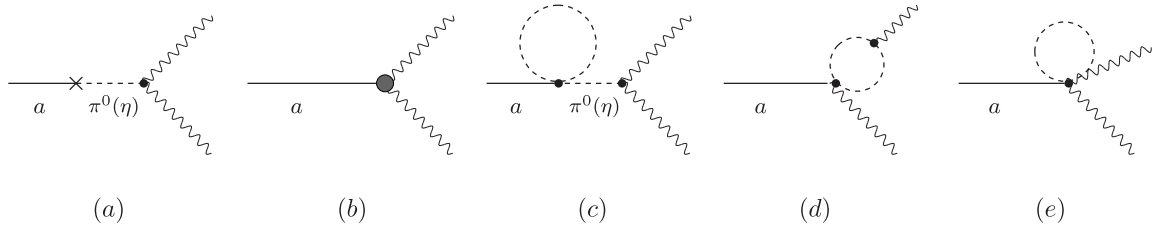

Figure 1. Feynman diagrams for the computation of the axion-photon coupling up to $\mathcal{O}\left(p^6\right)$. Here the dashed lines denote Goldstone bosons and wavy lines photons. Only pseudoscalar mesons are running in the loops.

where

$$f_\pm(\cos,\sin) = \sqrt{3}\left(\mu_{\pi^0}-\mu_\eta\right)\cos(3\epsilon) \pm 3\left(\mu_{K^0}-\mu_{K^+}\right)\sin\epsilon - \sqrt{3}\left(\mu_{K^0}+\mu_{K^+}-2\mu_{\pi^+}\right)\cos\epsilon - \frac{8M_{\pi^0}^2}{F_\pi^2\hat{m}}\left(3L_7^r+L_8^r\right)\left[2\sqrt{3}(\hat{m}-m_s)\cos\epsilon \pm 3\delta\sin\epsilon\right]. \tag{4.8}$$

The functions $f_\pm(\sin,\cos)$ are equivalent to $f_\pm(\cos,\sin)$ with the sine and the cosine interchanged, i.e., $f_\pm(\sin,\cos) = f_\pm(\cos\to\sin,\sin\to\cos)$, and ϵ is the LO pion-eta mixing angle in the vacuum as can be obtained by setting $\theta=0$ in the expression of ϵ_θ in eq. (2.8).

For the parameters C_7^W and C_8^W, it was argued in ref. [80] that C_7^W is largely suppressed compared to C_8^W as the latter receives a strong contribution from the η' while the former does not. The authors also suggested $|C_7^W| < 0.1|C_8^W|$. We use $\Gamma(\eta\to\gamma\gamma) = \frac{M_\eta^3}{64\pi}|T_\eta|^2$ with the $\eta\to\gamma\gamma$ amplitude given by [80]

$$T_\eta = \frac{e^2}{\sqrt{3}F_\pi}\left[\frac{F_\pi}{4\pi^2F_\eta}(1+x_\eta) - \frac{64}{3}M_\pi^3C_7^W + \frac{256}{3}(r-1)M_\pi^2\left(\frac{1}{6}C_7^W + C_8^W\right) + \mathcal{O}(m_s^2)\right] \tag{4.9}$$

to extract the value of C_8^W from the measured value of the $\eta\to\gamma\gamma$ width: $(0.516\pm 0.020)\,\mathrm{keV}$ [33]. Following ref. [80], we take $F_\eta = (118.4\pm 8.0)\,\mathrm{MeV}$ and assign a 30% uncertainty for the $\mathcal{O}\left(m_s^2\right)$ contribution compared to that of $\mathcal{O}\left(m_s\right)$, we get $C_8^W = (0.60\pm 0.20)\times 10^{-3}\,\mathrm{GeV}^{-2}$, as listed in table 1. We have set C_7^W to 0 as its effect can be absorbed into the uncertainty of C_8^W.

With the input parameters presented in table 1, one gets

$$g_{a\gamma\gamma} = \frac{\alpha_{\mathrm{em}}}{2\pi f_a}\left(\frac{\mathcal{E}}{\mathcal{C}} - 2.05(3)\right) = \left[0.197(3)\frac{\mathcal{E}}{\mathcal{C}} - 0.404(12)\right]\frac{m_a}{\mathrm{GeV}^2}. \tag{4.10}$$

The error for the axion-photon coupling is also dominated by the uncertainties of C_8^W, r and L_7^r, which are of similar size. From eq. (4.10), we obtain $g_{a\gamma\gamma}\simeq 1.2\times 10^{-16}\ldots 1.2\times 10^{-13}\,\mathrm{GeV}^{-1}$ for the axion mass in the range $1\ldots 1000\,\mu\mathrm{eV}$ with $\mathcal{E}/\mathcal{C}=8/3$. Especially for $m_a = 6.7\,\mu\mathrm{eV}$, this equation predicts $g_{a\gamma\gamma}\simeq 8.1\times 10^{-16}\,\mathrm{GeV}^{-1}$ for models with $\mathcal{E}/\mathcal{C}=8/3$ like the Dine-Fischler-Srednicki-Zhitnitsky (DFSZ) model [28], which is still in the allowed region by the recent axion dark matter search, with m_a around $6.7\,\mu\mathrm{eV}$ [84].

The Primakoff effect plays a key role in axion searches. For example, the working principle for an axion helioscope [85, 86] is that axions produced in the core of the Sun are converted back into photons in a strong magnetic field. Clearly, if the ratio $\mathcal{E}/\mathcal{C}=2$, which is

JHEP05(2020)001

N	$m_a\,[\mu\text{eV}\cdot\frac{10^{12}\,\text{GeV}}{f_a}]$	$(-\lambda_4)^{1/4}\,[10^{-2}\text{GeV}/f_a]$	$g_{a\gamma\gamma}^{\text{QCD}}\,[\frac{\alpha_{\text{em}}}{2\pi f_a}]$	$\chi_t^{1/4}\,[\text{MeV}]$	b_2
2 [53]	5.70(7)	5.79(10)	−1.92(4)	75.5(5)	−0.029(2)
3	5.71(9)	5.77(18)	−2.05(3)	75.6(6)	−0.028(3)

Table 2. Summary of the main numerical results of the present work shown in the third line. For comparison we also show the results in the second line obtained in the framework of the SU(2) CHPT [53]. For the axion-photon coupling $g_{a\gamma\gamma}$, only the model-independent part, denoted by $g_{a\gamma\gamma}^{\text{QCD}}$, is shown.

quite a possibility as shown by Kaplan in ref. [71], then the $g_{a\gamma\gamma}$ would be highly suppressed. The axion detection using the Primakoff effect, such as microwave cavity experiments, or light shining through wall experiments (for a recent review, see ref. [87]) would thus be extremely difficult. Here, we present the reference values of $g_{a\gamma\gamma}$ for $\mathcal{E}/\mathcal{C} = 2$ and 8/3:

$$g_{a\gamma\gamma} = \begin{cases} -0.06(4) \times 10^{-3}/f_a, & \mathcal{E}/\mathcal{C} = 2, \\ +0.71(4) \times 10^{-3}/f_a, & \mathcal{E}/\mathcal{C} = 8/3. \end{cases} \tag{4.11}$$

With the expressions of the axion mass and the axion-photon coupling, it is straightforward to estimate the axion lifetime, namely,

$$\tau_{a\to\gamma\gamma} = \frac{64\pi}{g_{a\gamma\gamma}^2 m_a^3} = \frac{3.4 \times 10^{54}\,\text{s}}{\left[\mathcal{E}/\mathcal{C} - 2.05(3)\right]^2}\left(\frac{\mu\text{eV}}{m_a}\right)^5. \tag{4.12}$$

As the axion lifetime is inversely proportional to m_a^5, the axion is more stable when its mass is smaller. The axion lifetime is estimated as $\tau_{a\to\gamma\gamma} \gtrsim 10^{33}\,\text{s}$ if the lower limit $f_a \gtrsim 0.5 \times 10^9\,\text{GeV}$ is employed. Such a cosmologically stable particle is a well-motivated cold dark matter candidate [32, 88].

5 Summary

In this paper, we have calculated the QCD θ-vacuum energy and in turn the axion potential up-to-and-including NLO corrections in SU(N) CHPT. Unlike the SU(2) case, no analytic solutions exist for SU(N) with $N \geq 3$. We work out for the first time a recursion relation for ϕ_f, up to an arbitrary order in θ. Then, as an extension of ref. [54], by expanding the one-loop effective generating functional around the free-field configuration in a θ-vacuum, we have calculated the θ-vacuum energy density up NLO, including the one-loop contribution, in SU(N) CHPT with N non-degenerate quark flavors. With the recursion relation for the ϕ_f angles, one can compute any-order cumulants of the QCD topological charge distribution as well as the axion mass and self-couplings.

Since the QCD axion potential as a function of a/f_a takes the same form as the QCD θ-vacuum energy as a function of θ, we have also calculated the axion mass and self-coupling to NLO from the SU(3) θ-vacuum energy density taking into account the strong isospin breaking effects. With the determination of the LECs from experimental data and

JHEP05(2020)001

lattice simulations, we have further evaluated the numerical values for axion mass and self-coupling up to NLO, which are similar to those obtained in the SU(2) case in ref. [53].

We also computed the axion-photon coupling up to $\mathcal{O}(p^6)$. Numerically, it is given by $g_{a\gamma\gamma} = \frac{\alpha_{\rm em}}{2\pi f_a}[\mathcal{E}/\mathcal{C} - 2.05(3)]$, which implies that if $\mathcal{E}/\mathcal{C} = 2$, the axion-photon coupling would be extremely small. In this case the axion searches using $g_{a\gamma\gamma}$, such as light shining through a wall or microwave cavity experiments, would be very difficult. This might also have an important impact on the axion electrodynamics as well as the possible existence of boson stars, in which the axion-photon coupling plays a crucial role.

Acknowledgments

The authors thank N.R. Acharya, S. Gonzàlez-Solís, M.-J. Yan and B.-S. Zou for useful discussions. F.-K.G. is grateful to the hospitality of the Helmholtz Institut für Strahlen- und Kernphysik where part of the work was done. M.-L.D. would like to thank the hospitality of the Institute of Theoretical Physics where part of the work was done. This work is supported in part by the China Postdoctoral Science Foundation (Grant No. 2017M620920), by NSFC and DFG through funds provided to the Sino-German Collaborative Research Center "Symmetries and the Emergence of Structure in QCD" (NSFC Grant No. 11621131001, DFG Grant No. TRR110), by NSFC (Grant No. 11835015 and No. 11947302), by the CAS Key Research Program of Frontier Sciences (Grant No. QYZDB-SSW-SYS013), by the CAS Center for Excellence in Particle Physics (CCEPP), and also by the Scientific Research Fund of Hunan Provincial Education Department (Grant No. 19C0772). The work of U.-G.M. was also supported in part by the CAS President's International Fellowship Initiative (PIFI) (Grant No. 2018DM0034), and by the VolkswagenStiftung (Grant No. 93562).

A Full solution of the vacuum angles for the SU(N) case

Let us derive the expressions of the vacuum angles ϕ_f, and thus the LO vacuum energy, to all orders of θ for SU(N) here. The starting equations are the SU(N) version of eqs. (2.10)

$$\begin{cases} m_f \sin\phi_f = \text{constant}, \\ \sum_{f=1}^{N} \phi_f = \theta. \end{cases} \tag{A.1}$$

We use the following expansions,

$$\begin{aligned} \sin\phi_f &= \sum_{n=0}^{\infty} s_{2n+1}\phi_f^{2n+1}, \quad \text{with } s_{2n+1} \equiv \frac{(-1)^n}{(2n+1)!}, \\ \phi_f &= \sum_{m=0}^{\infty} C_{f,2m+1}\theta^{2m+1}. \end{aligned} \tag{A.2}$$

Once we solve all the coefficients $C_{f,2m+1}$, we then get the general solution of ϕ_f. Let

$$m_f \sin\phi_f = \sum_{n=0}^{\infty} \alpha_{2n+1}\theta^{2n+1}, \tag{A.3}$$

then eqs. (A.1) are decomposed into equations for each odd order of θ.

JHEP05(2020)001

At $\mathcal{O}(\theta)$, one has

$$m_f C_{f,1} = \alpha_1, \quad \text{and} \quad \sum_{f=1}^{N} C_{f,1} = 1. \tag{A.4}$$

Thus, one gets

$$C_{f,1} = \frac{\bar{m}}{m_f} \tag{A.5}$$

with $\bar{m}$ defined in eq. (2.15).

At $\mathcal{O}(\theta^3)$, one has

$$C_{f,3} + s_3 C_{f,1}^3 = \frac{\alpha_3}{m_f}, \quad \text{and} \quad \sum_{f=1}^{N} C_{f,3} = 0, \tag{A.6}$$

the solution of which is

$$C_{f,3} = s_3 \left(\frac{\bar{m}}{m_f} \sum_{i=1}^{N} C_{i,1}^3 - C_{f,1}^3 \right). \tag{A.7}$$

Combining eqs. (A.5) and (A.7), one gets the known result in eq. (2.14).

At $\mathcal{O}(\theta^5)$, one has

$$C_{f,5} + 3 s_3 C_{f,1}^2 C_{f,3} + s_5 C_{f,1}^5 = \frac{\alpha_5}{m_f}, \quad \text{and} \quad \sum_{f=1}^{N} C_{f,5} = 0, \tag{A.8}$$

the solution of which is

$$C_{f,5} = 3 s_3 \left(\frac{\bar{m}}{m_f} \sum_{i=1}^{N} C_{i,1}^2 C_{i,3} - C_{f,1}^2 C_{f,3} \right) + s_5 \left(\frac{\bar{m}}{m_f} \sum_{i=1}^{N} C_{i,1}^5 - C_{f,1}^5 \right). \tag{A.9}$$

Notice that for the expansion of $\sin\phi_f$ in powers of θ in eq. (A.3), the terms at $\mathcal{O}(\theta^{2n+1})$ are closely related to the partition of $2n+1$ into odd parts (e.g., the partitions of 5 into odd parts include 5, $3+1+1$ and $1+1+1+1+1$, see the left side of eq. (A.8)) studied in number theory.

One can go to higher orders and solve for $C_{f,2n+1}$ in the same way. Finally, one gets the recursion relation for all the coefficients as

$$C_{f,2n+1} = \sum_{t=1}^{n} \sum_{(k_1,\ldots,k_t)} s_{K_t} \binom{K_t}{k_1,\ldots,k_t} \left[\frac{\bar{m}}{m_f} \sum_{i=1}^{N} \prod_{j=1}^{t} C_{i,2j-1}^{k_j} - \prod_{j=1}^{t} C_{f,2j-1}^{k_j} \right], \tag{A.10}$$

where k_j are nonnegative integers, $K_t \equiv \sum_{j=1}^{t} k_j$, $\sum_{(k_1,\ldots,k_t)}$ means that the sum runs over all possibilities of k_j satisfying $k_1 + \cdots + (2t-1)k_t = 2n+1$, and $\binom{K_t}{k_1,\ldots,k_t} = K_t!/(k_1! \cdots k_t!)$ are the multinomial coefficients.

JHEP05(2020)001

References

[1] R.J. Crewther, P. Di Vecchia, G. Veneziano and E. Witten, *Chiral Estimate of the Electric Dipole Moment of the Neutron in Quantum Chromodynamics*, *Phys. Lett.* **88B** (1979) 123 [*Erratum ibid.* **B 91** (1980) 487] [INSPIRE].

[2] C.A. Baker et al., *An Improved experimental limit on the electric dipole moment of the neutron*, *Phys. Rev. Lett.* **97** (2006) 131801 [hep-ex/0602020] [INSPIRE].

[3] W.C. Griffith, M.D. Swallows, T.H. Loftus, M.V. Romalis, B.R. Heckel and E.N. Fortson, *Improved Limit on the Permanent Electric Dipole Moment of ^{199}Hg*, *Phys. Rev. Lett.* **102** (2009) 101601 [arXiv:0901.2328] [INSPIRE].

[4] R.H. Parker et al., *First Measurement of the Atomic Electric Dipole Moment of ^{225}Ra*, *Phys. Rev. Lett.* **114** (2015) 233002 [arXiv:1504.07477] [INSPIRE].

[5] B. Graner, Y. Chen, E.G. Lindahl and B.R. Heckel, *Reduced Limit on the Permanent Electric Dipole Moment of ^{199}Hg*, *Phys. Rev. Lett.* **116** (2016) 161601 [*Erratum ibid.* **119** (2017) 119901] [arXiv:1601.04339] [INSPIRE].

[6] F.-K. Guo et al., *The electric dipole moment of the neutron from 2+1 flavor lattice QCD*, *Phys. Rev. Lett.* **115** (2015) 062001 [arXiv:1502.02295] [INSPIRE].

[7] nEDM collaboration, *Measurement of the permanent electric dipole moment of the neutron*, *Phys. Rev. Lett.* **124** (2020) 081803 [arXiv:2001.11966] [INSPIRE].

[8] R.D. Peccei and H.R. Quinn, *CP Conservation in the Presence of Instantons*, *Phys. Rev. Lett.* **38** (1977) 1440 [INSPIRE].

[9] R.D. Peccei and H.R. Quinn, *Constraints Imposed by CP Conservation in the Presence of Instantons*, *Phys. Rev.* **D 16** (1977) 1791 [INSPIRE].

[10] S. Weinberg, *A New Light Boson?*, *Phys. Rev. Lett.* **40** (1978) 223 [INSPIRE].

[11] F. Wilczek, *Problem of Strong P and T Invariance in the Presence of Instantons*, *Phys. Rev. Lett.* **40** (1978) 279 [INSPIRE].

[12] CAST collaboration, *Probing eV-scale axions with CAST*, *JCAP* **02** (2009) 008 [arXiv:0810.4482] [INSPIRE].

[13] Y. Inoue, Y. Akimoto, R. Ohta, T. Mizumoto, A. Yamamoto and M. Minowa, *Search for solar axions with mass around 1 eV using coherent conversion of axions into photons*, *Phys. Lett.* **B 668** (2008) 93 [arXiv:0806.2230] [INSPIRE].

[14] CAST collaboration, *New solar axion search using the CERN Axion Solar Telescope with ^{4}He filling*, *Phys. Rev.* **D 92** (2015) 021101 [arXiv:1503.00610] [INSPIRE].

[15] ADMX collaboration, *A SQUID-based microwave cavity search for dark-matter axions*, *Phys. Rev. Lett.* **104** (2010) 041301 [arXiv:0910.5914] [INSPIRE].

[16] E. Armengaud et al., *Axion searches with the EDELWEISS-II experiment*, *JCAP* **11** (2013) 067 [arXiv:1307.1488] [INSPIRE].

[17] J. Keller and A. Sedrakian, *Axions from cooling compact stars*, *Nucl. Phys.* **A 897** (2013) 62 [arXiv:1205.6940] [INSPIRE].

[18] A. Arvanitaki, M. Baryakhtar and X. Huang, *Discovering the QCD Axion with Black Holes and Gravitational Waves*, *Phys. Rev.* **D 91** (2015) 084011 [arXiv:1411.2263] [INSPIRE].

JHEP05(2020)001

[19] B.M. Brubaker et al., *First results from a microwave cavity axion search at 24 μeV*, *Phys. Rev. Lett.* **118** (2017) 061302 [arXiv:1610.02580] [INSPIRE].

[20] PandaX collaboration, *Limits on Axion Couplings from the First 80 Days of Data of the PandaX-II Experiment*, *Phys. Rev. Lett.* **119** (2017) 181806 [arXiv:1707.07921] [INSPIRE].

[21] CDEX collaboration, *Constraints on Axion couplings from the CDEX-1 experiment at the China Jinping Underground Laboratory*, *Phys. Rev.* **D 95** (2017) 052006 [arXiv:1610.07521] [INSPIRE].

[22] K. Ehret et al., *New ALPS Results on Hidden-Sector Lightweights*, *Phys. Lett.* **B 689** (2010) 149 [arXiv:1004.1313] [INSPIRE].

[23] OSQAR collaboration, *New exclusion limits on scalar and pseudoscalar axionlike particles from light shining through a wall*, *Phys. Rev.* **D 92** (2015) 092002 [arXiv:1506.08082] [INSPIRE].

[24] R. Bradley et al., *Microwave cavity searches for dark-matter axions*, *Rev. Mod. Phys.* **75** (2003) 777 [INSPIRE].

[25] M. Dine, W. Fischler and M. Srednicki, *A Simple Solution to the Strong CP Problem with a Harmless Axion*, *Phys. Lett.* **104B** (1981) 199 [INSPIRE].

[26] A.R. Zhitnitsky, *On Possible Suppression of the Axion Hadron Interactions* (in Russian), *Sov. J. Nucl. Phys.* **31** (1980) 260 [INSPIRE].

[27] J.E. Kim, *Weak Interaction Singlet and Strong CP Invariance*, *Phys. Rev. Lett.* **43** (1979) 103 [INSPIRE].

[28] M.A. Shifman, A.I. Vainshtein and V.I. Zakharov, *Can Confinement Ensure Natural CP Invariance of Strong Interactions?*, *Nucl. Phys.* **B 166** (1980) 493 [INSPIRE].

[29] J.E. Kim, *Light Pseudoscalars, Particle Physics and Cosmology*, *Phys. Rept.* **150** (1987) 1 [INSPIRE].

[30] G. Raffelt and D. Seckel, *Bounds on Exotic Particle Interactions from SN 1987a*, *Phys. Rev. Lett.* **60** (1988) 1793 [INSPIRE].

[31] J.E. Kim and G. Carosi, *Axions and the Strong CP Problem*, *Rev. Mod. Phys.* **82** (2010) 557 [*Erratum ibid.* **91** (2019) 049902] [arXiv:0807.3125] [INSPIRE].

[32] D.J.E. Marsh, *Axion Cosmology*, *Phys. Rept.* **643** (2016) 1 [arXiv:1510.07633] [INSPIRE].

[33] Particle Data Group collaboration, *Review of Particle Physics*, *Phys. Rev.* **D 98** (2018) 030001 [INSPIRE].

[34] L. Di Luzio, M. Giannotti, E. Nardi and L. Visinelli, *The landscape of QCD axion models*, arXiv:2003.01100 [INSPIRE].

[35] D.S.M. Alves and N. Weiner, *A viable QCD axion in the MeV mass range*, *JHEP* **07** (2018) 092 [arXiv:1710.03764] [INSPIRE].

[36] J. Preskill, M.B. Wise and F. Wilczek, *Cosmology of the Invisible Axion*, *Phys. Lett.* **120B** (1983) 127 [INSPIRE].

[37] L.F. Abbott and P. Sikivie, *A Cosmological Bound on the Invisible Axion*, *Phys. Lett.* **120B** (1983) 133 [INSPIRE].

[38] M. Dine and W. Fischler, *The Not So Harmless Axion*, *Phys. Lett.* **120B** (1983) 137 [INSPIRE].

JHEP05(2020)001

[39] L. Visinelli and P. Gondolo, *Dark Matter Axions Revisited*, *Phys. Rev.* **D 80** (2009) 035024 [arXiv:0903.4377] [INSPIRE].

[40] L. Visinelli and P. Gondolo, *Axion cold dark matter in view of BICEP2 results*, *Phys. Rev. Lett.* **113** (2014) 011802 [arXiv:1403.4594] [INSPIRE].

[41] K. Kaneta, H.-S. Lee and S. Yun, *Portal Connecting Dark Photons and Axions*, *Phys. Rev. Lett.* **118** (2017) 101802 [arXiv:1611.01466] [INSPIRE].

[42] P. Sikivie and Q. Yang, *Bose-Einstein Condensation of Dark Matter Axions*, *Phys. Rev. Lett.* **103** (2009) 111301 [arXiv:0901.1106] [INSPIRE].

[43] E.W. Kolb and I.I. Tkachev, *Axion miniclusters and Bose stars*, *Phys. Rev. Lett.* **71** (1993) 3051 [hep-ph/9303313] [INSPIRE].

[44] Y. Bai, V. Barger and J. Berger, *Hydrogen Axion Star: Metallic Hydrogen Bound to a QCD Axion BEC*, *JHEP* **12** (2016) 127 [arXiv:1612.00438] [INSPIRE].

[45] E. Braaten, A. Mohapatra and H. Zhang, *Dense Axion Stars*, *Phys. Rev. Lett.* **117** (2016) 121801 [arXiv:1512.00108] [INSPIRE].

[46] J. Eby, M. Leembruggen, P. Suranyi and L.C.R. Wijewardhana, *Collapse of Axion Stars*, *JHEP* **12** (2016) 066 [arXiv:1608.06911] [INSPIRE].

[47] D.G. Levkov, A.G. Panin and I.I. Tkachev, *Relativistic axions from collapsing Bose stars*, *Phys. Rev. Lett.* **118** (2017) 011301 [arXiv:1609.03611] [INSPIRE].

[48] L. Visinelli, S. Baum, J. Redondo, K. Freese and F. Wilczek, *Dilute and dense axion stars*, *Phys. Lett.* **B 777** (2018) 64 [arXiv:1710.08910] [INSPIRE].

[49] E. Braaten and H. Zhang, *Colloquium: The physics of axion stars*, *Rev. Mod. Phys.* **91** (2019) 041002.

[50] S. Weinberg, *Phenomenological Lagrangians*, *Physica* **A 96** (1979) 327 [INSPIRE].

[51] J. Gasser and H. Leutwyler, *Chiral Perturbation Theory to One Loop*, *Annals Phys.* **158** (1984) 142 [INSPIRE].

[52] J. Gasser and H. Leutwyler, *Chiral Perturbation Theory: Expansions in the Mass of the Strange Quark*, *Nucl. Phys.* **B 250** (1985) 465 [INSPIRE].

[53] G. Grilli di Cortona, E. Hardy, J. Pardo Vega and G. Villadoro, *The QCD axion, precisely*, *JHEP* **01** (2016) 034 [arXiv:1511.02867] [INSPIRE].

[54] F.-K. Guo and U.-G. Meißner, *Cumulants of the QCD topological charge distribution*, *Phys. Lett.* **B 749** (2015) 278 [arXiv:1506.05487] [INSPIRE].

[55] TWQCD collaboration, *Topological Susceptibility to the One-Loop Order in Chiral Perturbation Theory*, *Phys. Rev.* **D 80** (2009) 034502 [arXiv:0903.2146] [INSPIRE].

[56] V. Bernard, S. Descotes-Genon and G. Toucas, *Determining the chiral condensate from the distribution of the winding number beyond topological susceptibility*, *JHEP* **12** (2012) 080 [arXiv:1209.4367] [INSPIRE].

[57] F. Luciano and E. Meggiolaro, *Study of the theta dependence of the vacuum energy density in chiral effective Lagrangian models at zero temperature*, *Phys. Rev.* **D 98** (2018) 074001 [arXiv:1806.00835] [INSPIRE].

[58] M. Gorghetto and G. Villadoro, *Topological Susceptibility and QCD Axion Mass: QED and NNLO corrections*, *JHEP* **03** (2019) 033 [arXiv:1812.01008] [INSPIRE].

JHEP05(2020)001

[59] T. Vonk, F.-K. Guo and U.-G. Meißner, *Precision calculation of the axion-nucleon coupling in chiral perturbation theory*, *JHEP* **03** (2020) 138 [arXiv:2001.05327] [INSPIRE].

[60] G. Landini and E. Meggiolaro, *Study of the interactions of the axion with mesons and photons using a chiral effective Lagrangian model*, *Eur. Phys. J.* **C 80** (2020) 302 [arXiv:1906.03104] [INSPIRE].

[61] R. Brower, S. Chandrasekharan, J.W. Negele and U.J. Wiese, *QCD at fixed topology*, *Phys. Lett.* **B 560** (2003) 64 [hep-lat/0302005] [INSPIRE].

[62] N.R. Acharya, F.-K. Guo, M. Mai and U.-G. Meißner, *θ-dependence of the lightest meson resonances in QCD*, *Phys. Rev.* **D 92** (2015) 054023 [arXiv:1507.08570] [INSPIRE].

[63] S. Aoki and H. Fukaya, *Chiral perturbation theory in a theta vacuum*, *Phys. Rev.* **D 81** (2010) 034022 [arXiv:0906.4852] [INSPIRE].

[64] MILC collaboration, *Effects of nonequilibrated topological charge distributions on pseudoscalar meson masses and decay constants*, *Phys. Rev.* **D 97** (2018) 074502 [arXiv:1707.05430] [INSPIRE].

[65] J. Bijnens and J. Lu, *Technicolor and other QCD-like theories at next-to-next-to-leading order*, *JHEP* **11** (2009) 116 [arXiv:0910.5424] [INSPIRE].

[66] V. Bernard, S. Descotes-Genon and G. Toucas, *Topological susceptibility on the lattice and the three-flavour quark condensate*, *JHEP* **06** (2012) 051 [arXiv:1203.0508] [INSPIRE].

[67] J. Eby, M. Leembruggen, P. Suranyi and L.C.R. Wijewardhana, *QCD Axion Star Collapse with the Chiral Potential*, *JHEP* **06** (2017) 014 [arXiv:1702.05504] [INSPIRE].

[68] J. Bijnens and G. Ecker, *Mesonic low-energy constants*, *Ann. Rev. Nucl. Part. Sci.* **64** (2014) 149 [arXiv:1405.6488] [INSPIRE].

[69] S. Borsányi et al., *Calculation of the axion mass based on high-temperature lattice quantum chromodynamics*, *Nature* **539** (2016) 69 [arXiv:1606.07494] [INSPIRE].

[70] Flavour Lattice Averaging Group collaboration, *FLAG Review 2019: Flavour Lattice Averaging Group (FLAG)*, *Eur. Phys. J.* **C 80** (2020) 113 [arXiv:1902.08191] [INSPIRE].

[71] D.B. Kaplan, *Opening the Axion Window*, *Nucl. Phys.* **B 260** (1985) 215 [INSPIRE].

[72] G. Alonso-Álvarez, M.B. Gavela and P. Quilez, *Axion couplings to electroweak gauge bosons*, *Eur. Phys. J.* **C 79** (2019) 223 [arXiv:1811.05466] [INSPIRE].

[73] H. Georgi, D.B. Kaplan and L. Randall, *Manifesting the Invisible Axion at Low-energies*, *Phys. Lett.* **169B** (1986) 73 [INSPIRE].

[74] J. Wess and B. Zumino, *Consequences of anomalous Ward identities*, *Phys. Lett.* **37B** (1971) 95 [INSPIRE].

[75] E. Witten, *Global Aspects of Current Algebra*, *Nucl. Phys.* **B 223** (1983) 422 [INSPIRE].

[76] O. Kaymakcalan, S. Rajeev and J. Schechter, *Nonabelian Anomaly and Vector Meson Decays*, *Phys. Rev.* **D 30** (1984) 594 [INSPIRE].

[77] U.-G. Meißner, *Low-Energy Hadron Physics from Effective Chiral Lagrangians with Vector Mesons*, *Phys. Rept.* **161** (1988) 213 [INSPIRE].

[78] S. Scherer and M.R. Schindler, *A Primer for Chiral Perturbation Theory*, *Lect. Notes Phys.* **830** (2012) 1.

JHEP05(2020)001

[79] J. Bijnens, L. Girlanda and P. Talavera, *The Anomalous chiral Lagrangian of order p^6*, *Eur. Phys. J.* **C 23** (2002) 539 [hep-ph/0110400] [INSPIRE].

[80] K. Kampf and B. Moussallam, *Chiral expansions of the π^0 lifetime*, *Phys. Rev.* **D 79** (2009) 076005 [arXiv:0901.4688] [INSPIRE].

[81] J. Bijnens and K. Kampf, *Neutral pseudoscalar meson decays: $\pi^0 \to \gamma\gamma$ and $\eta \to \gamma\gamma$ in* SU(3) *limit*, *Nucl. Phys. Proc. Suppl.* **207-208** (2010) 220 [arXiv:1009.5493] [INSPIRE].

[82] J.F. Donoghue, B.R. Holstein and Y.C.R. Lin, *Chiral Loops in $\pi^0, \eta^0 \to \gamma\gamma$ and $\eta - \eta'$ Mixing*, *Phys. Rev. Lett.* **55** (1985) 2766 [*Erratum ibid.* **61** (1988) 1527] [INSPIRE].

[83] J. Bijnens, A. Bramon and F. Cornet, *Pseudoscalar Decays Into Photon-photon in Chiral Perturbation Theory*, *Phys. Rev. Lett.* **61** (1988) 1453 [INSPIRE].

[84] S. Lee, S. Ahn, J. Choi, B.R. Ko and Y.K. Semertzidis, *Axion Dark Matter Search around $6.7\,\mu eV$*, *Phys. Rev. Lett.* **124** (2020) 101802 [arXiv:2001.05102] [INSPIRE].

[85] P. Sikivie, *Experimental Tests of the Invisible Axion*, *Phys. Rev. Lett.* **51** (1983) 1415 [*Erratum ibid.* **52** (1984) 695] [INSPIRE].

[86] CAST collaboration, *New CAST Limit on the Axion-Photon Interaction*, *Nature Phys.* **13** (2017) 584 [arXiv:1705.02290] [INSPIRE].

[87] I.G. Irastorza and J. Redondo, *New experimental approaches in the search for axion-like particles*, *Prog. Part. Nucl. Phys.* **102** (2018) 89 [arXiv:1801.08127] [INSPIRE].

[88] M. Kawasaki and K. Nakayama, *Axions: Theory and Cosmological Role*, *Ann. Rev. Nucl. Part. Sci.* **63** (2013) 69 [arXiv:1301.1123] [INSPIRE].

JHEP05(2020)001